ORIGINAL RESEARCH

Rational design of multifunctional micelles against doxorubicin-sensitive and doxorubicin-resistant MCF-7 human breast cancer cells

Wei Hong[1]
Hong Shi[2]
Mingxi Qiao[3]
Xiang Gao[1]
Jie Yang[1]
Chunlian Tian[1]
Dexian Zhang[1]
Shengli Niu[1]
Mingchun Liu[1]

[1]Key Laboratory of Zoonosis of
Liaoning, College of Animal Science
and Veterinary Medicine, Shenyang
Agricultural University, Shenhe,
Shenyang, Liaoning, [2]Department of
Pharmaceutics, School of Pharmacy,
China Pharmaceutical University,
Jiangning, Nanjing, [3]Department of
Pharmaceutics, School of Pharmacy,
Shenyang Pharmaceutical University,
Shenyang, Liaoning, People's Republic
of China

Correspondence: Wei Hong
Key Laboratory of Zoonosis of Liaoning,
College of Animal Science and Veterinary
Medicine, Shenyang Agricultural University,
Dongling Road 120, Shenhe, Shenyang,
Liaoning 110866, People's Republic of
China
Tel/fax +86 24 8848 7156
Email hongwei_sy@163.com

Abstract: Even though a tremendous number of multifunctional nanocarriers have been developed to tackle heterogeneous cancer cells, little attention has been paid to elucidate how to rationally design a multifunctional nanocarrier. In this study, three individual functions (active targeting, stimuli-triggered release and endo-lysosomal escape) were evaluated in doxorubicin (DOX)-sensitive MCF-7 cells and DOX-resistant MCF-7/ADR cells by constructing four kinds of micelles with active-targeting (AT-M), passive-targeting, pH-triggered release ($_{pH}$T-M) and endo-lysosomal escape ($_{endo}$E-M) function, respectively. AT-M demonstrated the strongest cytotoxicity against MCF-7 cells and the highest cellular uptake of DOX due to the folate-mediated endocytosis. However, AT-M failed to exhibit the best efficacy against MCF-7/ADR cells, while $_{endo}$E-M exhibited the strongest cytotoxicity against MCF-7/ADR cells and the highest cellular uptake of DOX due to the lowest elimination of DOX from the cells. This was attributed to the carrier-facilitated endo-lysosomal escape of DOX, which avoided exocytosis by lysosome secretion, resulting in an effective accumulation of DOX in the cytoplasm. The enhanced elimination of DOX from the MCF-7/ADR cells also accounted for the remarkable decrease in cytotoxicity against the cells of AT-M. Three micelles were further evaluated with MCF-7 cells and MCF-7/ADR-resistant cells xenografted mice model. In accordance with the in vitro results, AT-M and $_{endo}$E-M demonstrated the strongest inhibition on the MCF-7 and MCF-7/ADR xenografted tumor, respectively. Active targeting and active targeting in combination with endo-lysosomal escape have been demonstrated to be the primary function for a nanocarrier against doxorubicin-sensitive and doxorubicin-resistant MCF-7 cells, respectively. These results indicate that the rational design of multifunctional nanocarriers for cancer therapy needs to consider the heterogeneous cancer cells and the primary function needs to be integrated to achieve effective payload delivery.

Keywords: rational design, multidrug resistance, active targeting, pH-triggered release, endo-lysosomal escape

Introduction

Cancer has become one of the most devastating diseases because of its complexity and heterogeneity, which allow the cancer cells to adapt to environment and evolve aggressively, leading to significant morbidity and mortality in patients.[1] Recently, multifunctional nanocarriers have been emerging as a promising approach to overcome the biologic complexity and heterogeneity during cancer chemotherapy.[2–5] The most distinguishing benefit of multifunctional nanocarriers is that they can be engineered to achieve targeted delivery of multiple therapeutic agents for multimodal chemotherapeutic strategies.[6]

The rationale of the multifunctional nanocarriers relies on the optimized pharmacokinetic and pharmacodynamic profiles of the encapsulated payloads by the passive and/or active targeting of the nanocarriers.[7] Passive targeting allows for the extravasation of the nanocarriers through the leaky cancer microvasculature and retention in the cancer interstitium or cells.[8–11] A newly reported liposome carrier, propylene glycol (PG), was made to load epirubicin (EPI), which enhanced EPI absorption in multidrug resistance (MDR) tumor cells to overcome the drug resistance.[12] Active targeting allows for the nanocarriers to selectively bind to receptors or antigens overexpressed on the surface of cancer cells and endocytosed by the cells.[13–15] In order to further increase the payload level inside the cancer cells, stimuli-triggered payload release was incorporated into the nanocarriers to achieve a controlled release pattern. Nanocarriers with triggered drug release mechanism in response to various physical or chemical stimuli such as high temperature,[16] pH[17] and ultrasound[18] have been developed to overcome the above-mentioned problem. Among these stimuli, pH sensitivity has been recognized as one of the best stimuli because of the easy and safe medical applications. A number of pH-responsive micelles based on poly(L-histidine) have been developed, such as poly(L-histidine) (polyHis, M_n 5K) poly(ethylene glycol) (PEG, M_n 2K) (PHis-PEG) diblock copolymer micelles,[19] the mixed micelles of PHis-PEG and poly(L-Lactide)-poly (ethylene glycol) (PLLA-PEG),[20] and the flower-like micelle constructed from poly(L-lactic acid) (PLA, M_n 3K)-poly(ethylene glycol) (PEG, M_n 2K)-poly(L-histidine) (polyHis, M_n 5K).[21] These micelles were found to undergo structural destabilization at slightly acidic pH due to the protonation of polyHis, which will provide an effective approach for bypassing P-glycoprotein (P-gp) efflux by rapid delivery of the cargoes into the cytosol. Moreover, multifunctional nanocarriers are engineered to have cancer targeting, sustained payload release, stimuli-triggered payload release and multiple payloads such as therapeutic agents, genes, cancer MDR reversal agents as well as imaging agents. For example, a multifunctional micellar nanocarrier was constructed by integrating folate-mediated targeting, acidic cancer pH-triggered release and endo-lysosomal escape for reversal of resistant MCF-7 cancer. The micelles showed greater cytotoxicity compared to folate-free micelles.[22] Wang et al designed and prepared a novel drug delivery system, designated S@L NPs, in which several smaller nanoparticles (NPs) are contained within a larger NP. S@L NPs could be triggered to degrade and release CS/PAA/VP-16 NPs in the acidic environment of the cytosol, endosomes or lysosomes, and CS/PAA/VP-16 NPs were capable of entering the nucleus

through nucleopores, which could enhance the anticancer effect of the loaded drug by inducing autophagy and apoptosis of MDR cells.[23] Multifunctional nanocarriers with active targeting, cell membrane translocation and pH-triggered payload release were developed for co-delivery of nucleic acids with traditional cytotoxic drugs.[24,25] These nanocarriers showed improved cellular uptake of nucleic acids and cytotoxic drugs, leading to the enhanced cytotoxicity against drug-resistant cancer cells. Applications of multifunctional nanocarriers to drug-sensitive cancer treatment have also burst onto a scene with better therapeutic efficacy.[26] Qu et al co-delivered chemotherapeutic drug (doxorubicin [DOX]) and small interfering RNA within a liposome to suppress the tumor growth.[27] Shi et al developed multifunctional star-shaped micelles by combining active targeting with redox-responsive payload release.[28] Dong et al constructed folate-conjugated and pH-responsive micelles loaded with vascular endothelial growth factor targeting small interfering RNA and DOX.[29]

Encouraged by the promise of multifunctional nanocarriers in addressing the heterogeneity of cancer, more and more effort has been put to develop various multifunctional micelles. However, little attention has been paid to elucidate how to rationally design a multifunctional nanocarrier against heterogeneous cancer cells. Although the rationale for using multifunctional micelles in cancer therapy is their ability to overcome the biologic barriers for intracellular payload delivery, the heterogeneity of cancer cells still needs to be considered. For example, the MDR cancer cells usually exhibit a significantly different intracellular microenvironment compared to sensitive cancer cells, such as overexpression of adenosine triphosphate (ATP)-dependent efflux pumps, enhanced compartmentalization, producing more serious challenge for payload delivery. Multifunctional nanocarriers for treating different cancer cells probably require a different design in order to achieve efficient payload delivery. Moreover, any advanced multifunctional nanocarrier should be started with a rationally basic design before integrating more functional parameters. Therefore, it was highly significant to shed some light on the following issues: 1) What are the primary functions of the multifunctional micelles for efficient payload delivery to drug-sensitive and drug-resistant cancer cells respectively? and 2) What is the difference between the multifunctional micelles for treating drug-sensitive and drug-resistant cancer cells? In this study, four kinds of micelles (AT-M/DOX, PT-M/DOX, $_{pH}$T-M/DOX and $_{endo}$E-M/DOX) were constructed to compare the effect of different functions on the therapeutic efficacy of MCF-7 and MCF-7/ADR cells

Table 1 Composition and functions of DOX-loaded polymeric micelles

Micelles	Composition (w/w)	Functional components
AT-M/DOX	Pluronic® F127/Pluronic® P123: 60/40, 20% Pluronic F127 conjugated with folate	Active targeting
PT-M/DOX	Pluronic F127/Pluronic P123: 60/40	Passive targeting
endoE-M/DOX	Pluronic F127/PHis-PLA-PEG-PLA-PHis: 50/50	Endo-lysosomal escape + passive targeting
pHT-M/DOX	Pluronic F127/Pluronic P123: 90/10	Simulated pH-triggered drug release

Abbreviation: DOX, doxorubicin.

in vitro and in vivo, respectively. The results indicated that effectively enhancing drug accumulation in the cancer cells is an ideal approach to design a multifunctional nanocarrier against MCF-7 sensitive cells, while endo-lysosomal escape plays a dominant role in sparing the payload elimination from MCF-7/ADR cells in order to achieve an effective delivery. The compositions and integrated functions of the micelles are summarized in Table 1.

Materials and methods
Materials

Doxorubicin hydrochloride (DOX·HCl) was purchased from Beijing HuaFeng United Technology Co., Ltd (Beijing, People's Republic of China). PEG (M_n: 2,000 g/mole), N,N'-carbonyldiimidazole,3-(4,5-dimethyl-thiazol-2-yl)-2,5-diphenyl-tetrazolium bromide (MTT) and Hoechst 33258 were purchased from Sigma (St Louis, MO, USA). Roswell Park Memorial Institute 1640 without folic acid and fetal bovine serum were purchased from Thermo Fisher Scientific (Waltham, MA, USA). LysoTracker Green was purchased from Beyotime® Biotechnology Co., Ltd (Nanjing, People's Republic of China). Pluronic F127 and Pluronic P123 were kindly supplied by BASF Ltd. (Shanghai, People's Republic of China). Purified deionized water was prepared by the Milli-Q plus system (EMD Millipore, Billerica, MA, USA). All the other reagents and chemicals were of analytical or chromatographic grade and were purchased from Concord Technology (Tianjin, People's Republic of China).

Cell culture

The human breast cancer cell line MCF-7 was purchased from American Type Culture Collection (ATCC, Manassas, VA, USA). The MCF-7/DOX-resistant cell line was established from parental MCF-7 and supplied by KeyGen Biotech. Co., Ltd (Nanjing, People's Republic of China). The drug-resistant index of the MCF-7/DOX-resistant cell line was 54. Culture plates and dishes were purchased from Corning Incorporated (Corning, NY, USA). MCF-7 cells were cultured in Roswell Park Memorial Institute 1640 medium without folic acid, supplemented with 10% fetal bovine serum, 100 IU/mL penicillin and 100 µg/mL streptomycin sulfate. MCF-7/ADR cells were cultured in the same medium with the addition of 1,000 ng/mL of DOX. All the cells were cultured at 37°C in a humidifier with 5% CO₂ atmosphere. All the experiments were performed on the cells in the logarithmic phase of growth.

Animals

Female BALB/c nude mice (20±2 g, 4–6 weeks old), supplied by the Department of Experimental Animals of Shenyang Pharmaceutical University (Shenyang, People's Republic of China), were acclimated at 25°C and 55% of humidity under natural light/dark conditions. The mice were fed with food containing no folic acid for 2 weeks prior to the study and for the duration of the study. The ethics committee of Shenyang Pharmaceutical University approved this study, and all animal experiments were carried out in accordance with the guidelines evaluated and approved by the committee.

Tested formulations

DOX·HCl solution: doxorubicin hydrochloride solution; AT-M/DOX: DOX-incorporated micelles composed of Pluronic F127 (20% of Pluronic F127 conjugated with folate) and Pluronic P123 (w/w: 60/40) with active targeting; PT-M/DOX: DOX-incorporated micelles composed of Pluronic F127 and Pluronic P123 (w/w: 60/40) with passive targeting function; endoE-M/DOX: DOX-incorporated micelles composed of PHis-PLA-PEG-PLA-PHis and Pluronic F127 (w/w: 50/50) with endo-lysosomal escape; pHT-M/DOX: DOX-incorporated micelles composed of Pluronic P123 and Pluronic F127 (w/w: 90/10). pHT-M/DOX was developed to simulate the micelles with pH-triggered release function. The DOX concentration of the tested formulation was 2 mg/mL.

Synthesis and characterization of PHis-PLA-PEG-PLA-PHis and folate-Pluronic F127 copolymers

The copolymers used in this work were custom-made with reference to our previous publications.[22,30,31]

Preparation and characterization of DOX-loaded micelles

DOX was incorporated into the micelles by thin-film hydration method. First, DOX·HCl (30 mg) was stirred overnight with triethylamine (molar ratio, 1/3) in acetonitrile (60 mL) to obtain the DOX base. The solvent was removed by rotary evaporator at 40°C for 2 h and then chloroform was added to extract DOX base. After the extraction, chloroform was evaporated by rotary evaporator at 40°C for 2 h. The vacuum was further applied to remove the residual solvent at room temperature overnight. The DOX base (20 mg) was blended with 180 mg of different copolymer mixtures in 20 mL of acetonitrile and sonicated for 30 min. The solvent was evaporated by rotary evaporator at 50°C to obtain a thin film. Residual acetonitrile in the film was completely removed under vacuum at room temperature overnight. The resultant thin film was hydrated with 10 mL of phosphate-buffered saline (PBS; pH 7.4) for 30 min to obtain DOX-incorporated micellar suspension. The suspension was filtered through a 0.22 μm membrane filter to remove the unincorporated DOX aggregates. The blank micelles were prepared as described above without adding DOX base.

The hydrodynamic diameter and particle size distribution of the micelles were measured by dynamic light scattering (DLS; Zetasizer Naso ZS; Malvern Instruments, Malvern, UK). All the measurements were carried out at 25°C after equilibration for 5 min. All the micellar solutions were filtered through a 0.45 μm disposable membrane filter prior to measurement. All the values were the average of at least three independent samples.

Transmission electron microscopy (TEM) pictures of the copolymer micelles were captured on a transmission electron microscope (JEM-1230; Akishima, Tokyo, Japan) operating at an acceleration voltage of 80 KV without staining. Micellar samples were prepared by dipping a copper grid into the micellar solution. A few minutes after the deposition, the extra solution of the copper grid was blotted away with a strip of filter paper. The copper grid was air-dried at room temperature for 2 h before TEM observation.

The drug loading coefficient (DL%) and the encapsulation efficiency (EE%) of DOX-incorporated micellar solution were measured by a multifunctional microplate reader (Tecan, Männedorf, Switzerland) with the wavelength set at 480 nm. Ultracentrifugation method was applied to separate the free DOX from micelles. DOX-incorporated micelles (5 mL) were centrifuged for 60 min at 20,000 rpm (4°C) followed by filtration through 0.45 μm filters. The weight-free DOX was determined by measuring the absorption of

supernatant. Total weight of DOX in micelles was determined by measuring the absorption of the samples after dissolution of the micelles with 2 mL of acetonitrile. The total weight of DOX-incorporated micelles was obtained by freeze drying the micelles. The EE% was assayed as the ratio of the amount of drug encapsulated in micelles to the total weight of the drug in micelles. The DL% was assayed as the ratio of the weight of DOX encapsulated in micelles to the total weight of the DOX-incorporated micelles. DL% and EE% were calculated according to the following equations, respectively:

$$EE\% = \frac{\text{Weight of the drug in micelles}}{\text{Weight of the feeding drug}} \times 100$$

$$DL\% = \frac{\text{Weight of the drug in micelles}}{\text{Weight of the feeding copolymers and drug}} \times 100$$

Modulated differential scanning calorimetry (MDSC)

Thermal properties of the micelles were observed by MDSC. Samples weighing 3–5 mg were analyzed with an MDSC Q2000 (TA Instrument, New Castle, DE, USA) in sealed aluminum pans. The flowing rate of N_2 was controlled at 50 mL/min. The samples were cooled to −20°C and heated to 250°C with a heating rate of 20°C/min. The samples were prepared by lyophilizing the Pluronic F127 micellar solution, PHis-PLA-PEG-PLA-PHis micellar solution, physical mixture of Pluronic F127 and PHis-PLA-PEG-PLA-PHis micellar solution and Pluronic F127/PHis-PLA-PEG-PLA-PHis mixed micellar solution. The heating–cooling cycle was conducted twice. The melting point (T_m) and the glass transition temperature (T_g) were obtained on the reversing heat flow of the second heating–cooling cycle.

In vitro drug release from the copolymer micelles

The in vitro DOX release from the copolymer micelles was studied using a dialysis bag (molecular weight cutoff size 3,500 Da) under sink conditions. Aliquots of DOX-incorporated micelles (3.0 mL) were transferred into the dialysis bags and dialyzed against 80 mL of phosphate buffers (pH 7.4 and 5.5) containing 0.5% (v/v) Tween-80 at 37°C, respectively. At predetermined time intervals, 0.2 mL aliquots were withdrawn and replaced with an equal volume of fresh medium. The concentration of DOX was measured using a multifunctional microplate reader (Tecan) with the wavelength set at 480 nm. The in vitro release experiments

were conducted in triplicate at each pH value. The in vitro DOX release profiles were plotted with cumulative drug release as a function of time.

In vitro cell cytotoxicity

In vitro cytotoxicity against MCF-7 and MCF-7/ADR cells of DOX-incorporated micelles was assessed by a standard MTT assay.[32] MCF-7 cells and MCF-7/ADR cells were seeded in 96-well plates at a density of 5×10^3 cells per well and incubated for 24 h, respectively. The growth medium was replaced with fresh medium containing an indicated concentration (0.5, 1, 2, 4, 6, 8, 10 and 12 µg/mL for MCF-7 cancer cells; 1, 5, 10, 50, 100, 150, 200 and 300 µg/mL for MCF-7/ADR cancer cells) of the tested formulations (AT-M/DOX, $_{pH}$T-M/DOX, $_{endo}$E-M/DOX, PT-M/DOX and DOX solution). Control wells were treated with an equivalent volume of DOX-free medium. The cells were incubated at 37°C for 24 h. After incubation, the wells were rinsed with PBS, which was followed by addition of MTT solution (5 mg/mL) to each well. The plates were further incubated for 4 h, allowing the viable cells to reduce the yellow MTT into purple formazan crystals. After incubation, the medium was removed completely and the purple formazan crystals were dissolved by adding 150 µL of dimethyl sulfoxide. The absorbance was measured at 570 nm using a multifunctional microplate reader (Tecan). The half maximal inhibitory concentration (IC_{50}) values were calculated using nonlinear regression analysis, and the MDR reversal effect was assessed by quantifying the IC_{50} values of the tested formulations.

Clonogenic cell survival assay in monolayer

Clonogenic cell survival assay was performed as previously described with modifications.[33] Briefly, MCF-7 and MCF-7/ADR cancer cells were seeded in six-well plates at a density of 400 cells in 2 mL of medium per well, respectively. After 6 h of incubation, the cells were treated with 2 mL of the tested formulations (AT-M/DOX, $_{pH}$T-M/DOX, $_{endo}$E-M/DOX, PT-M/DOX and DOX solution) at IC_{50} concentration. After 24 h, the medium was discarded to stop treatment and replaced by 2 mL of DOX-free medium. After 14 days of incubation at 37°C in a humidifier with 5% CO_2 atmosphere, the cells were stained with crystal violet and colonies up to 50 cells were counted. Plating efficiency, surviving fraction and colony mean size were determined for each condition.

Flow cytometry

MCF-7 cells and MCF-7/ADR cells were seeded at a density of 1×10^5 cells/well in six-well plates and incubated for

24 h to allow for cell attachment, respectively. The cells were incubated with 1 µg/mL of DOX solution and DOX-incorporated micelles (AT-M/DOX, PT-M/DOX, $_{pH}$T-M/DPX and $_{endo}$E-M/DOX) for 2 h, respectively. After incubation, the cells were rinsed with ice-cold PBS three times. The cells were harvested by trypsinization and centrifuged at 1,000 rpm for 5 min. The cells were resuspended in 500 µL of PBS medium and analyzed for cellular uptake of DOX using a BD FACS Caliber flow cytometer (FACSCAN; Becton Dickinson, San Jose, CA, USA). To measure exocytosis of DOX, the cells were rinsed with cold PBS after incubation with 1 µg/mL of DOX solution and DOX-incorporated micelles (AT-M/DOX, PT-M/DOX, $_{pH}$T-M/DOX and $_{endo}$E-M/DOX) for 2 h, respectively. Then fresh medium (DOX-free cell culture) was added immediately. At different time intervals (0, 0.5, 1, 2, 3, 4, 6 and 8 h), the cells were prepared as described above and the intracellular concentration of DOX was determined using BD FACS Calibur flow cytometer (FACSCAN, Becton Dickinson).

Confocal laser scanning microscope (CLSM)

MCF-7/ADR cells were seeded on cover-slide system at a density of 2.5×10^4 cells/well in a humidifier with 5% CO_2 atmosphere for 24 h at 37°C. Different formulations (AT-M/DOX, PT-M/DOX, $_{pH}$T-M/DPX, $_{endo}$E-M/DOX and DOX solution) containing 1 µg/mL of DOX were added to the medium and incubated with the cells for 1, 2, 4 and 8 h, respectively. After incubation, the cells were washed three times with cold PBS and stained with 50 nM LysoTracker Green for 30 min to visualize the endosomes/lysosomes and with 10 µM Hoechst 33258 for 10 min to visualize the nuclei, respectively. Then the cells were fixed with 4% paraformaldehyde for 30 min. The microscopic images were captured using a CLSM (FV1000-IX81; Olympus Corporation, Tokyo, Japan).

Antitumor efficacy of DOX-incorporated micelles

The antitumor efficacy was investigated with MCF-7 (drug-sensitive cancer cell line) and MCF-7/ADR (drug-resistant cancer cell line) xenografted BALB/c nude mice, respectively. MCF-7 cells and MCF-7/ADR cells were transplanted into female BALB/c nude mice by subcutaneous injection of 1×10^7 cells in the right rare flanks of the mice, respectively. When the tumor volume reached 50–100 mm³, administration was started and the day was considered as day 0. At day 0, the mice were randomly divided into five groups (seven mice

Table 2 The exact dose of encapsulated DOX in the micelles and free DOX in the solution

Formulations	AT-M/DOX (mg)	PT-M/DOX (mg)	endoE-M/DOX (mg)	DOX·HCl solution (mg)
Encapsulated DOX[a]	2.124	2.136	2.178	N/A
Free DOX[b]	0.017	0.019	0.008	2.400
Total	2.141	2.155	2.186	2.400

Notes: [a]Encapsulated DOX = $0.2 \times C_{DOX} \times EE\% \times 6$, C_{DOX} is the DOX concentration in micelles. [b]Free DOX = $0.2 \times C_{DOX} \times (1-EE\%) \times 6$. AT-M/DOX: DOX-incorporated micelles composed of Pluronic F127 (20% of Pluronic F127 conjugated with folate) and Pluronic P123 (w/w: 60/40) with active targeting. PT-M/DOX: DOX-incorporated micelles composed of Pluronic F127 and Pluronic P123 (w/w: 60/40) with passive targeting function. endoE-M/DOX: DOX-incorporated micelles composed of PHis-PLA-PEG-PLA-PHis and Pluronic F127 (w/w: 50/50) with endo-lysosomal escape.
Abbreviations: DOX, doxorubicin; DOX·HCl, doxorubicin hydrochloride; N/A, not available; EE, encapsulation efficiency.

per group). They were treated six times (days 0, 3, 6, 9, 12, 15) at a 3-day interval with 0.2 mL of AT-M/DOX, PT-M/DOX, endoE-M/DOX, DOX·HCl solution (physiological saline as the transport buffer) and physiological saline, respectively. All the formulations were injected intravenously through the tail vein at a dose of 10 mg/kg. The calculated exact dose of DOX encapsulated in the micelles and free DOX in the solution (free DOX) is shown in Table 2. The tumor volume and the body weight of the mice were measured every 2 days. At the end of the experiment (day 22), all mice were sacrificed and the tumors were harvested and weighed. The antitumor activity was assessed with the tumor volume (V), which was calculated by the following equation:

$$V(mm^3) = LW^2/2$$

where length (L) was the longest diameter and width (W) was the shortest diameter perpendicular to length. To calculate the tumor growth inhibition (TGI), the tumor volumes at day 22 were recorded and calculated by the following equation:

$$TGI = 1 - \frac{(V_{22} - V_0)_{formulation\ in\ group}}{(V_{22} - V_0)_{control\ group}}$$

where V_0 is the volume of the tumor on day 0 and V_{22} is the volume of the tumor on day 22.

Statistical analysis
All experiments were performed at least three times and the quantitative data were presented as the mean ± standard deviation (SD). Statistical comparisons were determined by analysis of variance or Student's t-test. P-values <0.05 and <0.01 were considered statistically significant.

Results and discussion
Construction and characterization of different micelles
To elucidate the primary functions of the multifunctional micelles for efficient payload delivery to MCF-7 and

MCF-7/ADR cells, four kinds of micelles with different functional components were constructed to compare their therapeutic effect against the cells, respectively. Passive targeting micelles (PT-M/DOX) were composed of Pluronic F127 and Pluronic P123 with a weight ratio of 60/40, while the active targeting micelles (AT-M/DOX) were constructed with the same composition as PT-M/DOX, except that 20% of Pluronic F127 was conjugated with folate. Endo-lysosomal escape micelles (endoE-M/DOX) were composed of Pluronic F127 and PHis-PLA-PEG-PLA-PHis with a weight ratio of 50/50. PHis-PLA-PEG-PLA-PHis was used to facilitate the endo-lysosomal escape of DOX. The weight ratio of the two copolymers was carefully adjusted to ensure similar DOX release from the micelles in order to eliminate the effect caused by different DOX concentrations in the cells (Figure 1A). pH-triggered release micelles were simulated by constructing the micelles (pHT-M) with faster DOX release (Figure 1A). pHT-M composed of Pluronic F127 and Pluronic P123 with a weight ratio of 90/10 showed similar drug release profile as that of pHendoSM/DOX at pH 5.5 (Figure 1B). pHendoSM/DOX micelles which are capable of simulating the pH-triggered drug release at pH 5.5 were used in our previous study.[22] pHT-M micelles were developed instead of the pH-sensitive micelles because the PHis-PLA-PEG-PLA-PHis–based pH-sensitive micelles featured both pH-triggered DOX release and endo-lysosomal escape functions.

The DOX-incorporated micelles were characterized in terms of size and size distribution, morphology, surface charge, DL% as well as EE%. The corresponding results are summarized in Table 3. The DLS measurements showed that the average diameters of DOX-loaded mixed micelles were all close to 100 nm, with good polydispersity indexes <0.1. The size and morphology of the DOX-incorporated micelles were also measured by TEM. As presented in Figure 2, smooth spherical morphology and uniform size distribution were observed for the micelles with the particle size that correlated well with those measured by DLS. The particle size is an important parameter for intracellular payload delivery because small-sized micelles (<200 nm) are beneficial to
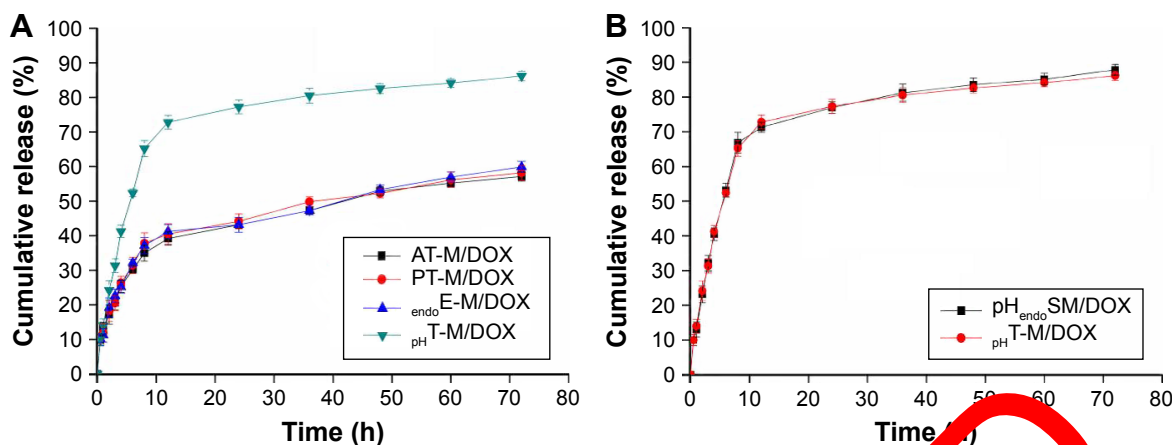
Figure 1 In vitro DOX release profiles from AT-M/DOX, PT-M/DOX, endoE-M/DOX and pHT-M/DOX at pH 7.4 (**A**) and pH 5.5 (**B**). The concentration of the copolymer mixture was 10 mg/mL (mean ± SD, n=6).
Notes: AT-M/DOX: DOX-incorporated micelles composed of Pluronic F127 (20% of Pluronic F127 conjugated with folate) and Pluronic P123 (w/w: 60/40) with active targeting. PT-M/DOX: DOX-incorporated micelles composed of Pluronic F127 and Pluronic P123 (w/w: 60:40) with passive targeting function. endoE-M/DOX: DOX-incorporated micelles composed of PHis-PLA-PEG-PLA-PHis and Pluronic F127 (w/w: 50/50) with endo-lysosomal escape. pHT-M/DOX: DOX-incorporated micelles composed of Pluronic P123 and Pluronic F127 (w/w: 90/10).
Abbreviations: DOX, doxorubicin; SD, standard deviation.

the low-level reticuloendothelial system uptake, leading to effective enhanced permeability and retention effect for passive targeting.[34] All the micelles exhibited similar slightly negative surface charge at pH 7.4, indicating a good steric protection. The nearly net surface charge of the micelles was able to prevent the recognition of opsonin, leading to prolonged in vivo circulation and subsequent passive or active targeting. The four DOX-incorporated micelles showed similar DL% and EE%, that is, around 9% and 99%, respectively. The relatively high EE% of DOX in the micelles could be achieved due to the low solubility of DOX base in phosphate buffer (28.25 µg/mL) as well as its good compatibility with the inner core of micelles. The low solubility of DOX base also indicates a successful conversion of DOX·HCl salt to free base with the addition of triethylamine.

Microstructure characterization of the mixed micelles

When two different copolymers are applied to form mixed micelles, the co-micellization of them needs to be

characterized to exclude the possibility of forming the mixture of two mono-copolymer micelles.[35] In this study, MDSC was applied to verify the co-micellization of PHis-PLA-PEG-PLA-PHis and Pluronic F127. The thermograms of Pluronic F127 mono-micelles, PHis-PLA-PEG-PLA-PHis mono-micelles, Pluronic F127/PHis-PLA-PEG-PLA-PHis mixed micelles (50/50, w/w) and their physical mixture counterpart (50/50, w/w) are shown in Figure 3. The Pluronic F127 mono-micelles showed endothermic peak at 44.5°C, which was attributed to the melting of PEO block.[35] The PHis-PLA-PEG-PLA-PHis mono-micelles revealed two endothermic peaks at 59.6°C and 188.3°C, which were assigned to the melting of PEG block and glass transition of PHis-PLA block, respectively. The physical mixture of Pluronic F127 and PHis-PLA-PEG-PLA-PHis mono-micelles demonstrated the same endothermic peaks as their mono-micelles. However, the Pluronic F127/PHis-PLA-PEG-PLA-PHis mixed micelles showed two endothermic peaks at 47.8°C and 54.2°C, corresponding to the melting of PEO block and PEG blocks, respectively. In addition, the glass transition

Table 3 The physicochemical characterization of DOX-incorporated micelles (n=3)

Formulations	Particle size (nm)	ξ potential (mV)	PDI	DL%	EE%
endoE-M/DOX	105.4±10.4	−5.97±0.12	0.078±0.004	9.07±0.14	99.6±0.84
AT-M/DOX	96.3±8.2	−5.56±0.08	0.071±0.006	8.85±0.12	99.2±1.04
pHT-M/DOX	108.6±9.8	−5.24±0.09	0.081±0.005	8.99±0.12	99.5±0.91
PT-M/DOX	92.1±7.6	−5.38±0.11	0.095±0.009	8.91±0.11	99.1±0.83

Notes: AT-M/DOX: DOX-incorporated micelles composed of Pluronic F127 (20% of Pluronic F127 conjugated with folate) and Pluronic P123 (w/w: 60/40) with active targeting. PT-M/DOX: DOX-incorporated micelles composed of Pluronic F127 and Pluronic P123 (w/w: 60:40) with passive targeting function. endoE-M/DOX: DOX-incorporated micelles composed of PHis-PLA-PEG-PLA-PHis and Pluronic F127 (w/w: 50/50) with endo-lysosomal escape. pHT-M/DOX: DOX-incorporated micelles composed of Pluronic P123 and Pluronic F127 (w/w: 90/10).
Abbreviations: DL, drug loading; DOX, doxorubicin; EE, encapsulation efficiency; PDI, polydispersity index.
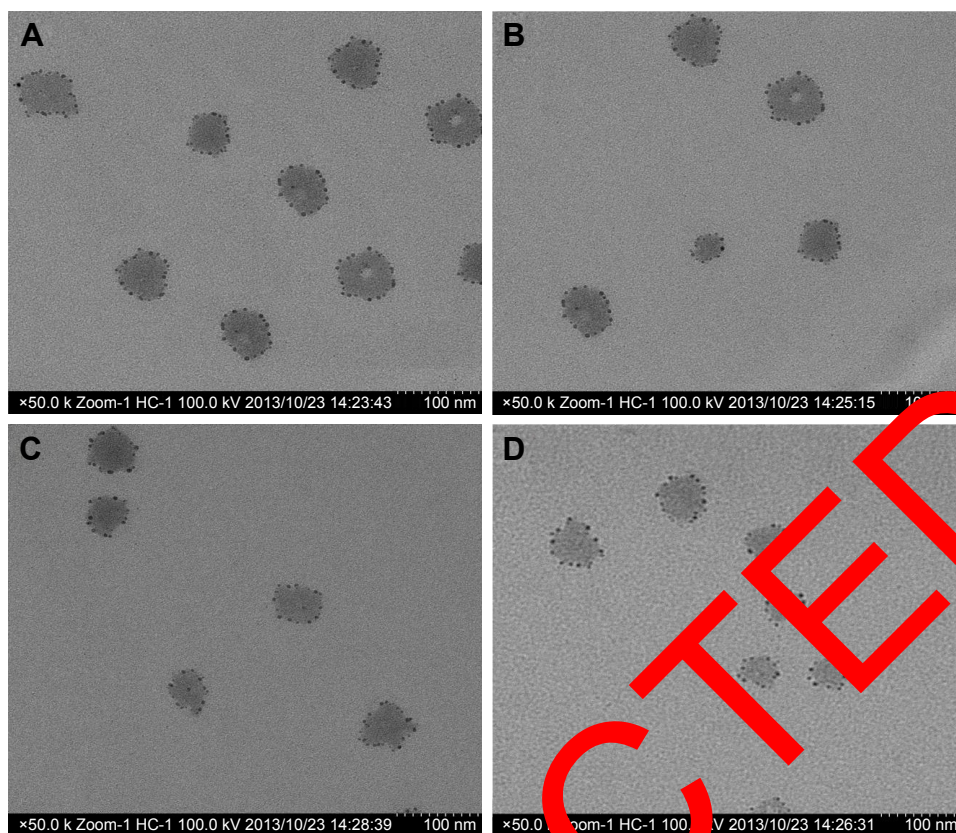
Figure 2 TEM images of AT-M/DOX (**A**), PT-M/DOX (**B**), endoE-M/DOX (**C**) and pHT-M/DOX (**D**).
Notes: AT-M/DOX: DOX-incorporated micelles composed of Pluronic F127 (20% of Pluronic F127 conjugated with folate) and Pluronic P123 (w/w: 60/40) with active targeting. PT-M/DOX: DOX-incorporated micelles composed of Pluronic F127 and Pluronic P123 (w/w: 60/40) with passive targeting function. endoE-M/DOX: DOX-incorporated micelles composed of PHis-PLA-PEG-PLA-PHis and Pluronic F127 (w/w: 50/50) with endo-lysosomal escape. pHT-M/DOX: DOX-incorporated micelles composed of Pluronic P123 and Pluronic F127 (w/w: 90/10).
Abbreviations: DOX, doxorubicin; TEM, transmission electron microscopy.
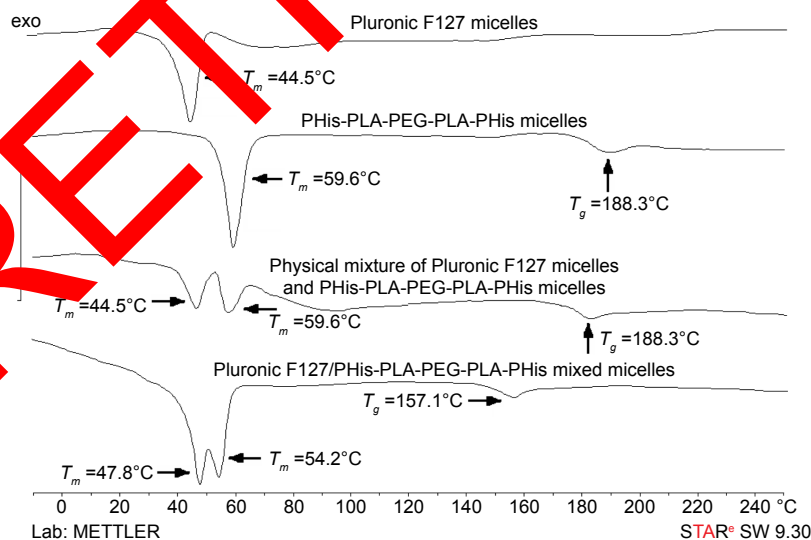
Figure 3 Reversing endothermic curves of Pluronic® F127 micelles, PHis-PLA-PEG-PLA-PHis micelles, physical mixture of Pluronic® F127 micelles and PHis-PLA-PEG-PLA-PHis micelles (w/w: 5/5) and Pluronic® F127/PHis-PLA-PEG-PLA-PHis mixed micelles (w/w: 5/5).
Notes: AT-M/DOX: DOX-incorporated micelles composed of Pluronic F127 (20% of Pluronic F127 conjugated with folate) and Pluronic P123 (w/w: 60/40) with active targeting. PT-M/DOX: DOX-incorporated micelles composed of Pluronic F127 and Pluronic P123 (w/w: 60/40) with passive targeting function. endoE-M/DOX: DOX-incorporated micelles composed of PHis-PLA-PEG-PLA-PHis and Pluronic F127 (w/w: 50/50) with endo-lysosomal escape. pHT-M/DOX: DOX-incorporated micelles composed of Pluronic P123 and Pluronic F127 (w/w: 90/10).
Abbreviations: PEG, poly(ethylene glycol); PLA, poly(L-lactic acid).

endothermic peak of PHis-PLA block was shifted to lower temperature of 157.1°C. The change in the endothermic peaks could be attributed to the intertwist of two hydrophilic blocks (PEO and PEG) and hydrophobic blocks (PPO and PHis-PLA).[36] The results indicate the co-micellization of Pluronic F127 and PHis-PLA-PEG-PLA-PHis, resulting in the formation of mixed micelles.

The co-micellization of Pluronic F127 and Pluronic P123 was characterized using DLS because the Pluronic copolymers showed similar endothermic behavior. Pluronic F127 and Pluronic P123 showed remarkable difference in the particle size of the micelles. Pluronic F127 is a more hydrophilic copolymer with relatively short PPO blocks and long PEO blocks, forming micelles with small particle size around 40 nm. But Pluronic P123 is a more hydrophobic copolymer with relatively long PPO blocks and short PEO blocks, forming micelles with much bigger particle size (~110 nm) than Pluronic F127 (Figure 4). The average particle size of mixed micelles of Pluronics was 90 nm when the weight ratio of Pluronic P123/Pluronic F127 was 90/10, which fell in the range between the particle size of Pluronic F127 micelles and Pluronic P123 micelles. The median particle size and the relatively narrow size distribution polydispersity (polydispersity index < 0.1) of the mixed micelles indicates the co-micellization of two Pluronics.[35]

In vitro cytotoxicity and cellular uptake of different micelles

The in vitro cytotoxicity of the four DOX-incorporated micelles was first studied against MCF-7/ADR and MCF-7 cells using MTT assay with DOX solution as control. The MDR characteristic of the MCF-7/ADR cells wa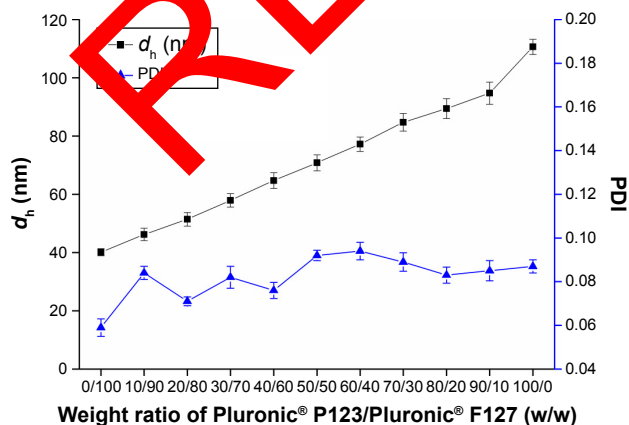s confirmed by the invisible cytotoxicity of DOX solution in a wide concentration range. The inhibition of four DOX-incorporated micelles on the MCF-7 and MCF-7/ADR cells is shown in Figure 5A and B, respectively. Compared to DOX solution, all the micelles exhibited higher IC_{50} value against MCF-7 cells due to the sustained release pattern of DOX and different cellular uptake pathway. Among the micelles, AT-M/DOX showed the lowest IC_{50} value, followed by $_{pH}$T-M/DOX, $_{endo}$E-M/DOX and PT-M/DOX (Figure 5A). Considering the DOX release profile from AT-M/DOX, which is similar to those of $_{endo}$E-M/DOX and PT-M/DOX, the strongest cytotoxicity of AT-M/DOX was clearly attributed to enhanced endocytosis due to folate-mediated targeting. AT-M/DOX still exhibited a moderately lower IC_{50} value, even though the DOX release from the micelles was much lower than $_{pH}$T-M/DOX, indicating the dominant role of folate-mediated active targeting in killing drug-sensitive MCF-7 cells. Compared to DOX solution, all the micelles exhibited significantly lower IC_{50} value against MCF-7/ADR cells due to the endocytic pathway into the cells that bypassed the efflux by ATP binding cassette (ABC) transporters. Among the micelles, $_{endo}$E-M/DOX exhibited the lowest IC_{50} value against MCF-7/ADR cells, followed by $_{pH}$T-M/DOX, AT-M/DOX and PT-M/DOX (Figure 5B). It is worth noting that two micelles (AT-M/DOX and $_{endo}$E-M/DOX) demonstrated remarkably different performance between the MCF-7 and MCF-7/ADR cells. AT-M/DOX with the strongest cytotoxic activity against MCF-7 cells failed to exhibit the same inhibitory effect against MCF-7/ADR cells, exhibiting no significant IC_{50} value with the other two micelles ($_{pH}$T-M/DOX and PT-M/DOX) despite the folate-mediated endocytosis. $_{endo}$E-M/DOX with the strongest cytotoxic activity against MCF-7/ADR cells failed to exhibit the same inhibitory effect against MCF-7 cells, demonstrating no significant IC_{50} value with PT-M/DOX. These results indicate that active targeting and endosomal escape function play a dominant role in killing MCF-7 cells and MCF-7/ADR cells, respectively.

However, the MTT assay measures the metabolic activity linked to mitochondrial function, which does not always correlate with the cell viability after treatment. This assay dose not differentiate between cytotoxic and cytostatic effects.[37] Cancer cells can proliferate during the interval between treatments, leading to treatment failure. In this regard, evaluation of the efficacy of functional micelles that may reduce this repopulation can be performed by the clonogenic assay, which determines the ability of a cell line to proliferate and form colonies.[38] The clonogenic assay is the gold standard for measuring cell survival after treatment with drugs. For this
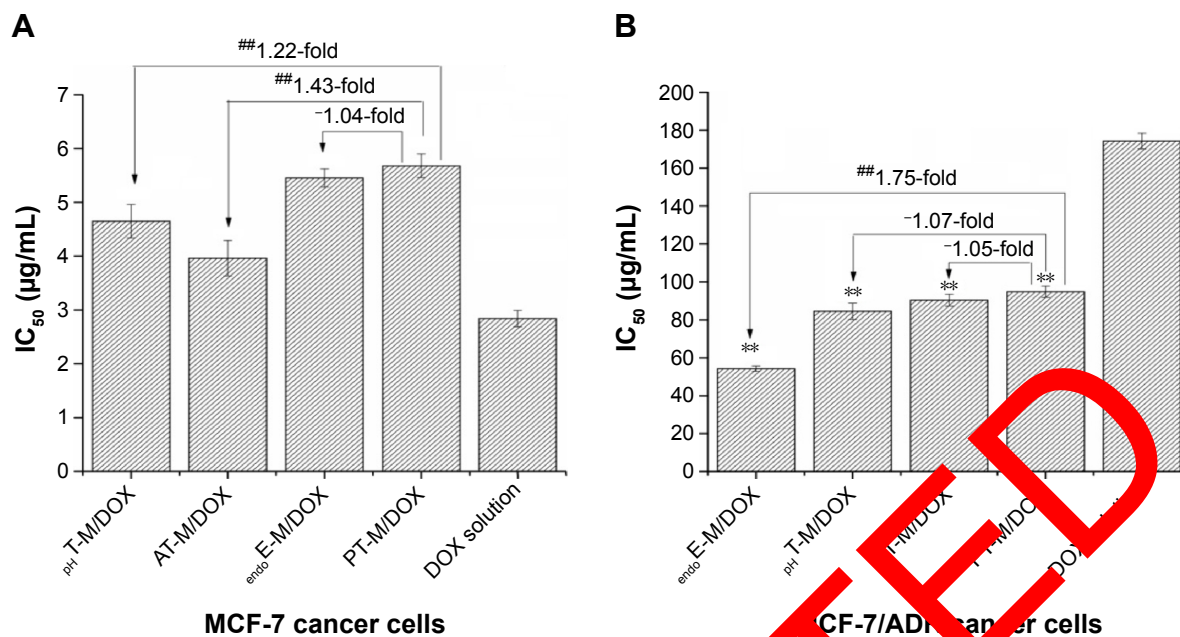

Figure 4 The hydrodynamic diameter (d_h) and PDI of mixed micelles as a function of Pluronic® F127/Pluronic® P123 weight ratio (mean ± SD, n=6).
Abbreviations: PDI, polydispersity index; SD, standard deviation.

Figure 5 In vitro cytotoxicity of DOX solution, AT-M/DOX, $_{endo}$E-M/DOX, $_{pH}$T-M/DOX and PT-M/DOX against MCF-7 cancer cells (**A**) and MCF-7/ADR cells (**B**) after 24 h incubation.
Notes: **$P<0.01$: significantly different from the DOX solution, ##$P<0.01$: significantly different from PT-M/DOX, −$P>0$: not significantly different from PT-M/DOX.
AT-M/DOX: DOX-incorporated micelles composed of Pluronic F127 (20% of Pluronic F127 conjugated with folate) and Pluronic P123 (w/w: 60/40) with active targeting. PT-M/DOX: DOX-incorporated micelles composed of Pluronic F127 and Pluronic P123 (w/w: 60/40) with passive targeting function. $_{endo}$E-M/DOX: DOX-incorporated micelles composed of PHis-PLA-PEG-PLA-PHis and Pluronic F127 (w/w: 50/50) with endo-lysosomal escape. $_{pH}$T-M/DOX: DOX-incorporated micelles composed of Pluronic P123 and Pluronic F127 (w/w: 90/10).
Abbreviation: DOX, doxorubicin.

purpose, AT-M/DOX, $_{pH}$T-M/DOX, $_{endo}$E-M/DOX, PT-M/DOX and DOX solution were further tested at clonogenic MCF-7 and MCF-7/ADR cell lines. Figure 6 shows the effects of the tested formulations at IC$_{50}$ concentration on the clonogenic survival of MCF-7 and MCF-7/ADR cancer cells. Over 14 days of the experiment, pretreatment of MCF-7 cells with AT-M/DOX for 24 h significantly reduced the survival of colonies (approximately 88% reduction). However, pretreatment with $_{endo}$E-M/DOX for 24 h did not reduce the formation in comparison with AT-M/DOX, indicating that $_{endo}$E-M/DOX showed less effect against MCF-7 cancer cells. While for MCF-7/ADR cells, the relative number of colonies was reduced by 3% with $_{endo}$E-M/DOX, 31% with $_{pH}$T-M/DOX, 46% with AT-M/DOX, 51% with PT-M/DOX and 63% with the DOX solution after pretreatment for 24 h, respectively. AT-M/DOX was less effective in reducing the proliferation of MCF-7/ADR clonogenic cells. The results correlated well with those obtained by MTT assay.

The cellular uptake of the four DOX-incorporated micelles by MCF-7 and MCF-7/ADR cells was evaluated using flow cytometry. As shown in Figure 7, AT-M/DOX showed the strongest intracellular DOX fluorescence intensity, followed by $_{pH}$T-M/DOX, $_{endo}$E-M/DOX and PT-M/DOX in MCF-7

cells (Figure 7A). $_{endo}$E-M/DOX exhibited the strongest intracellular DOX fluorescence intensity, followed by $_{pH}$T-M/DOX, AT-M/DOX and PT-M/DOX among the micelles in MCF-7/ADR cells (Figure 7B). The effect of the different micelles on the cellular uptake of DOX was further evaluated using CLSM with DOX solution as control. The subcellular distribution of DOX in MCF-7 and MCF-7/ADR cells is shown in Figure 8A and B, respectively. AT-M/DOX revealed stronger DOX staining inside the cells than the other three micelles ($_{pH}$T-M/DOX, $_{endo}$E-M/DOX and PT-M/DOX) at different incubation time points, indicating the micelles with active targeting showed a faster and more efficient accumulation of DOX within the cells than the other micelles. After 0.5 h of incubation, AT-M/DOX showed an obvious DOX staining on the nuclear periphery as characterized by the red fluorescence around the nucleus, resulting in many cells appearing as a void halo (Figure 7A). With the incubation time increased to 2 h, DOX staining was mainly localized throughout the nucleoplasm with the depletion of "halo" nuclei. In addition, the nuclei were surrounded by cytoplasm that was diminished to a rim within which light punctuate of DOX staining was occasionally found. The DOX staining of all the micelles increased with incubation time and reached a plateau level
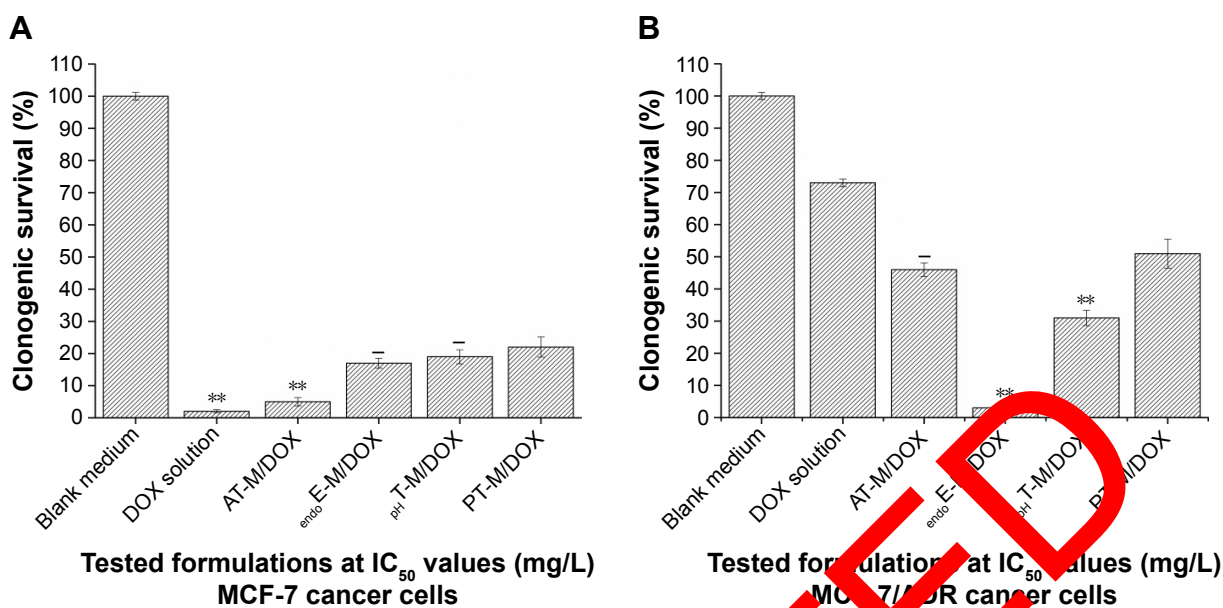
Figure 6 Effects of AT-M/DOX, $_{pH}$T-M/DOX, $_{endo}$E-M/DOX, PT-M/DOX and DOX solution at IC$_{50}$ concentration on the clonogenic survival of MCF-7 (**A**) and MCF-7/ADR (**B**) cancer cells.

Notes: Data present the mean plus SD percentage of clonogenic survival compared with control (blank medium) obtained from three independent experiments in triplicate. **$P<0.01$: significantly different from PT-M/DOX, $^-P>0.05$: not significantly different from PT-M/DOX. AT-M/DOX: DOX-incorporated micelles composed of Pluronic F127 (20% of Pluronic F127 conjugated with folate) and Pluronic P123 (w/w: 60/40) with active targeting. T-M/DOX: DOX-incorporated micelles composed of Pluronic F127 and Pluronic P123 (w/w: 60:40) with passive targeting function. $_{endo}$E-M/DOX: DOX-incorporated micelles composed of PHis-PLA-PEG-PLA-PHis and Pluronic F127 (w/w: 50/50) with endo-lysosomal escape. $_{pH}$T-M/DOX: DOX-incorporated micelles composed of Pluronic P123 and Pluronic F127 (w/w: 90/10).

Abbreviations: DOX, doxorubicin; SD, standard deviation; IC$_{50}$, half maximal inhibitory concentration.

at 2 h, which was much longer than that of DOX solution due to the sustained release profile of DOX. Compared to MCF-7 cells, MCF-7/ADR cells demonstrated a remarkable difference in the DOX subcellular distribution after incubation with the formulations. $_{endo}$E-M/DOX revealed a broader DOX distribution and stronger DOX staining in the MCF-7/ADR cells than the other three micelles (AT-M/DOX, $_{pH}$T-M/DOX and PT-M/DOX), indicating that micelles with endo-lysosomal escape showed more efficient accumulation of DOX within the cells than the other micelles. $_{endo}$E-M/DOX showed DOX staining of nuclei at 0.5 h and increased with incubation. The staining reached the highest intensity and broadest distribution at 2 h. Compared to $_{endo}$E-M/DOX, $_{pH}$T-M/DOX, AT-M/DOX and PT-M/DOX showed pockets of DOX intensity and a localized DOX intensity distribution along with a few dot shapes of fluorescence inside the cells. In addition, DOX solution revealed an incapability of accumulation in the MCF-7/ADR cells as characterized by the invisible DOX staining inside the cells.

Cellular elimination of DOX in MCF-7 and MCF-7/ADR cells

The different results of in vitro cytotoxicity and cellular uptake between MCF-7 and MCF-7/ADR cells were probably

attributed to the enhanced cellular elimination by MCF-7/MDR cells. In order to verify this hypothesis, the cellular elimination of DOX from MCF-7 and MCF-7/ADR cells was further studied by flow cytometry, respectively (Figure 9). All the tested micelles showed decreased intracellular accumulation of DOX in MCF-7 and MCF-7/ADR cells with increase in time. However, the elimination profiles of DOX from the two cells were remarkably different. The elimination of DOX from MCF-7 cells delivered by different micelles was similar and fairly low (Figure 9A). Almost 70% of the DOX still remained in the cells after 8 h of incubation (Figure 9A). This was further confirmed by quite a low amount of DOX present in the medium (data not shown). However, the elimination of DOX from MCF-7/ADR cells was remarkably accelerated, except that delivered by $_{endo}$E-M/DOX (Figure 9B). Less than 20% of the DOX was retained in the cells after 8 h of incubation with FA-M/DOX, FR-M/DOX and plain-M/DOX, which was much lower than that retained on incubation with $_{endo}$E-M/DOX (Figure 9B). Therefore, the different elimination profiles of AT-M/DOX and $_{endo}$E-M/DOX from the MCF-7 and MCF-7/ADR cells explain their difference in performance in cytotoxicity and cellular uptake.

The enhanced elimination profile of DOX from MCF-7/ADR cells could be attributed to the resistance
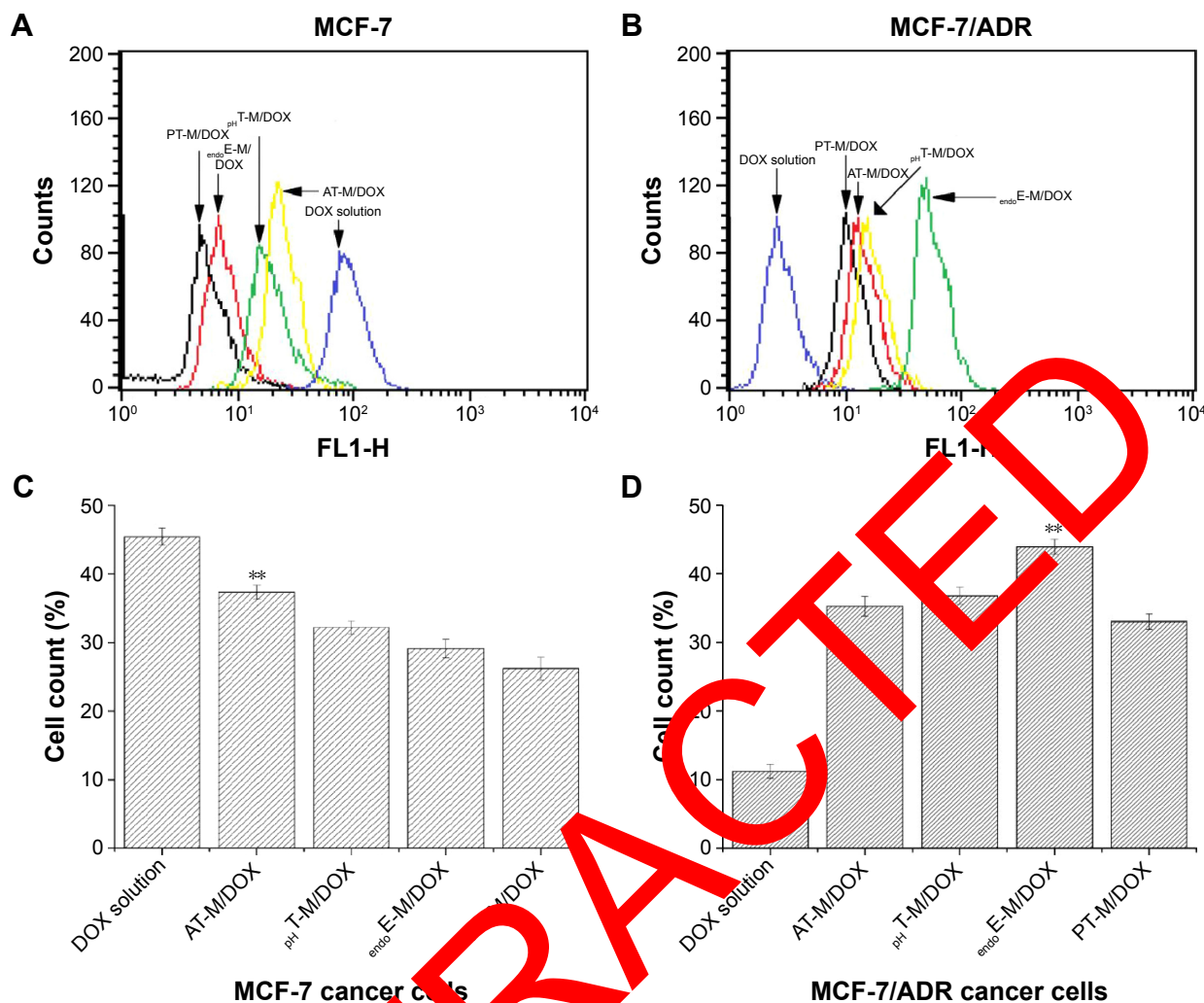
Figure 7 The cellular uptake of MCF-7 cells (**A**) and MCF-7/ADR cells (**B**); quantitative data for the cellular uptake of MCF-7 cells (**C**) and MCF-7/ADR cells (**D**) incubated with DOX solution, AT-M/DOX, endoE-M/DOX, pHT-M/DOX and PT-M/DOX for 2 h at 37°C.
Notes: **$P<0.01$: significantly different from pHT-M/DOX. AT-M/DOX: DOX-incorporated micelles composed of Pluronic F127 (20% of Pluronic F127 conjugated with folate) and Pluronic P123 (w/w: 60/40) with active targeting. PT-M/DOX: DOX-incorporated micelles composed of Pluronic F127 and Pluronic P123 (w/w: 60/40) with passive targeting function. endoE-M/DOX: DOX-incorporated micelles composed of PHis-PLA-PEG-PLA-PHis and Pluronic F127 (w/w: 50/50) with endo-lysosomal escape. pHT-M/DOX: DOX-incorporated micelles composed of Pluronic P123 and Pluronic F127 (w/w: 90/10).
Abbreviations: DOX, doxorubicin; FL1-H, height of fluorescence intensity.

phenotype of the cells. As compared to sensitive cell lines, drug-resistant cells usually display overexpression of the ABC transporters such as P-gp and enhanced intracellular sequestration, leading to a decreased accumulation of drug in the cells. NP-like micelles have been demonstrated to be internalized into cells by the endocytic pathway and translocated in either endosomes or lysosomes, which bypassed the efflux by ABC transporters and resulted in higher intracellular accumulation.[39] DOX became protonated in the acidic endo-lysosomes, making it difficult to diffuse across the endo-lysosomal membrane, and was entrapped in the compartments. Even though little is known about the exocytosis of nanoparticles from drug-resistant cells, considering

lysosome secretion as one of the main pathways for exocytosis, the enhanced sequestration in the compartments probably led to the exocytosis as in early endosomes or lysosomes. This explained the faster elimination of DOX from FA-M/DOX, FR-M/DOX and plain-M/DOX than that from endoE-M/DOX. The low elimination of DOX from endoE-M/DOX was attributed to the copolymer-facilitated endo-lysosomal escape of DOX, which avoided the excytosis by lysosome secretion. The P-gp might also contribute to the efflux of DOX in the cytoplasm after endo-lysosomal escape because endoE-M/DOX showed moderately faster elimination of DOX from MCF-7/ADR cells than that from MCF-7 cells, as characterized by lower intracellular DOX after 8 h of incubation.
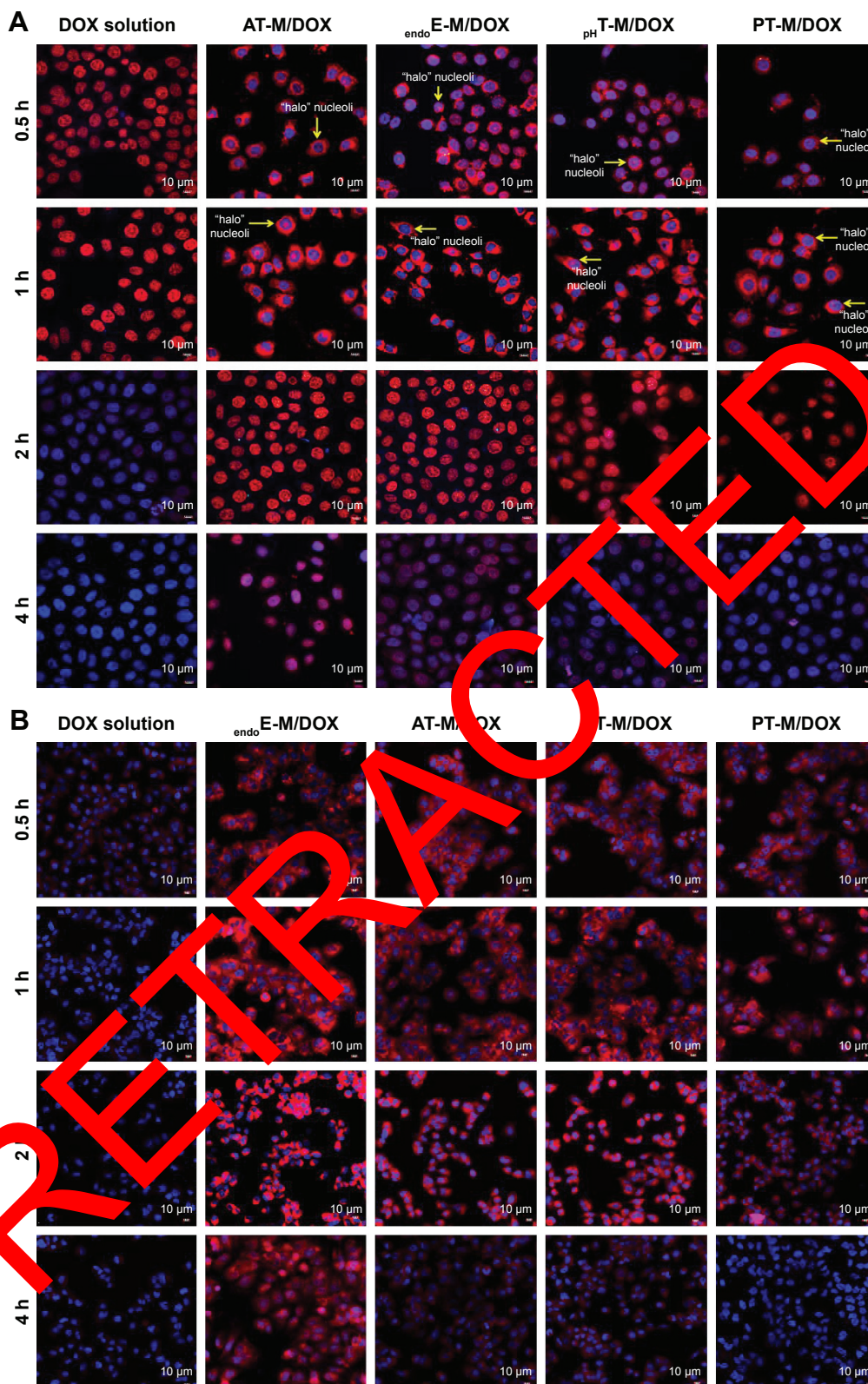
Figure 8 The confocal microscopic images of AT-M/DOX, $_{pH}$T-M/DOX, $_{endo}$E-M/DOX, PT-M/DOX and DOX solution in MCF-7 cells (**A**) and MCF-7/ADR cells (**B**) after 0.5, 1, 2 and 4 h of incubation at 37°C.

Notes: The cells were double labeled with the nucleus selective dye (Hoechst 33258, blue) and anticancer drug (DOX, red). AT-M/DOX: DOX-incorporated micelles composed of Pluronic F127 (20% of Pluronic F127 conjugated with folate) and Pluronic P123 (w/w: 60/40) with active targeting. PT-M/DOX: DOX-incorporated micelles composed of Pluronic F127 and Pluronic P123 (w/w: 60/40) with passive targeting function. $_{endo}$E-M/DOX: DOX-incorporated micelles composed of PHis-PLA-PEG-PLA-PHis and Pluronic F127 (w/w: 50/50) with endo-lysosomal escape. $_{pH}$T-M/DOX: DOX-incorporated micelles composed of Pluronic P123 and Pluronic F127 (w/w: 90/10).
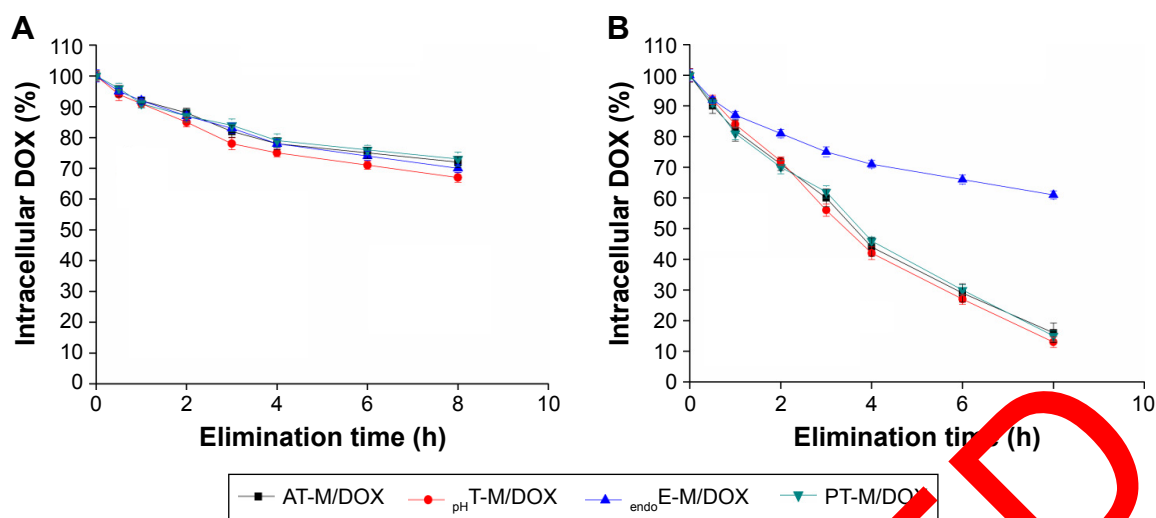
Abbreviation: DOX, doxorubicin.

Figure 9 The amount of intracellular DOX in AT-M/DOX, $_{pH}$T-M/DOX, $_{endo}$E-M/DOX and PT-M/DOX at different elimination time periods in MCF-7 cancer cells (**A**) and MCF-7/ADR cancer cells (**B**) (n=6).
Notes: AT-M/DOX: DOX-incorporated micelles composed of Pluronic F127 (20% of Pluronic F127 conjugated with folate) and Pluronic P123 (w/w: 60/40) with active targeting. PT-M/DOX: DOX-incorporated micelles composed of Pluronic F127 and Pluronic P123 (w/w: 60/40) with passive targeting function. $_{endo}$E-M/DOX: DOX-incorporated micelles composed of PHis-PLA-PEG-PLA-PHis and Pluronic F127 (w/w: 50/50) with endosomal escape. $_{pH}$T-M/DOX: DOX-incorporated micelles composed of Pluronic P123 and Pluronic F127 (w/w: 90/10).
Abbreviation: DOX, doxorubicin.

These results indicate that payloads delivered by NPs such as micelles also can be efficiently eliminated by the MCF-7/ADR cells. The enhanced sequestration in endo-lysosomes is a major cellular barrier for effective intracellular accumulation of payloads.

Endo-lysosomal escape of DOX from MCF-7 and MCF-7/ADR cancer cells

The low elimination of DOX from MCF-7/ADR cells delivered by $_{endo}$E-M/DOX was probably due to the endosomal escape facilitated by the "proton sponge" effect of PHis blocks in the copolymer.[29–32,40,41] $_{endo}$E-M/DOX-facilitated endo-lysosomal escape of DOX was further studied using CLSM with double labeling. The endosomes and lysosomes were selectively stained with LysoTracker Green, which was a specific marker for the acidic organelles. The red fluorescence of DOX colocalization with the green fluorescence of the acidic organelle dye would reveal a yellow fluorescence. As shown in Figure 10A, the MCF-7/ADR cells revealed an overwhelming majority of yellow fluorescence when the cells were incubated with $_{endo}$E-M/DOX, AT-M/DOX, $_{pH}$T-M/DOX and PT-M/DOX for 1 h, demonstrating that these micelles entered into the cells by the endocytic pathway. After 8 h of incubation, the cells incubated with $_{endo}$E-M/DOX showed an evident dissociation of red fluorescence with the green fluorescence and broader cytoplasmic distribution of DOX, as compared to the others displaying disappearance of red fluorescence.[42] The enhanced red fluorescence of DOX in

the cytoplasm indicates the effective endo-lysosomal escape of DOX facilitated by $_{endo}$E-M/DOX. The disappearance of red fluorescence of DOX indicates exocytosis of the endo-lysosomal content or drug degradation in the lysosomes due to ineffective endo-lysosomal escape.[43] In addition, the green fluorescence of the endo-lysosomes became weaker during the incubation, indicating the change in acidity in the endo-lysosomal environment as a result of the proton sponge effect of PHis because the staining of the endosomes or lysosomes by the tracker was dependent on the acidity of the compartments.[21,44,45] As compared to MCF-7/ADR cells, the MCF-7 cells demonstrated a time-dependent increase in the red fluorescence of DOX and broader cytoplasmic distribution during 8 h of incubation with all micelles (Figure 10B). This indicates that DOX was capable of escaping from the endo-lysosomes without the aid of nanocarrier-facilitated endosomal escape in the MCF-7 cells.

Overall, the in vitro cellular results indicate the significance of the individual functional parameters in treating DOX-sensitive and DOX-resistant cancer cells. 1) Active targeting has been demonstrated to be an effective approach to increase cellular uptake of NPs, leading to enhanced DOX accumulation and cytotoxicity against DOX-sensitive cancer cells. However, active targeting failed to produce effective DOX accumulation and cytotoxicity against DOX-resistant cancer cells due to the enhanced cellular elimination from the cells after folate-mediated endocytosis. 2) Endosomal escape has been demonstrated to be an effective approach to avoid the
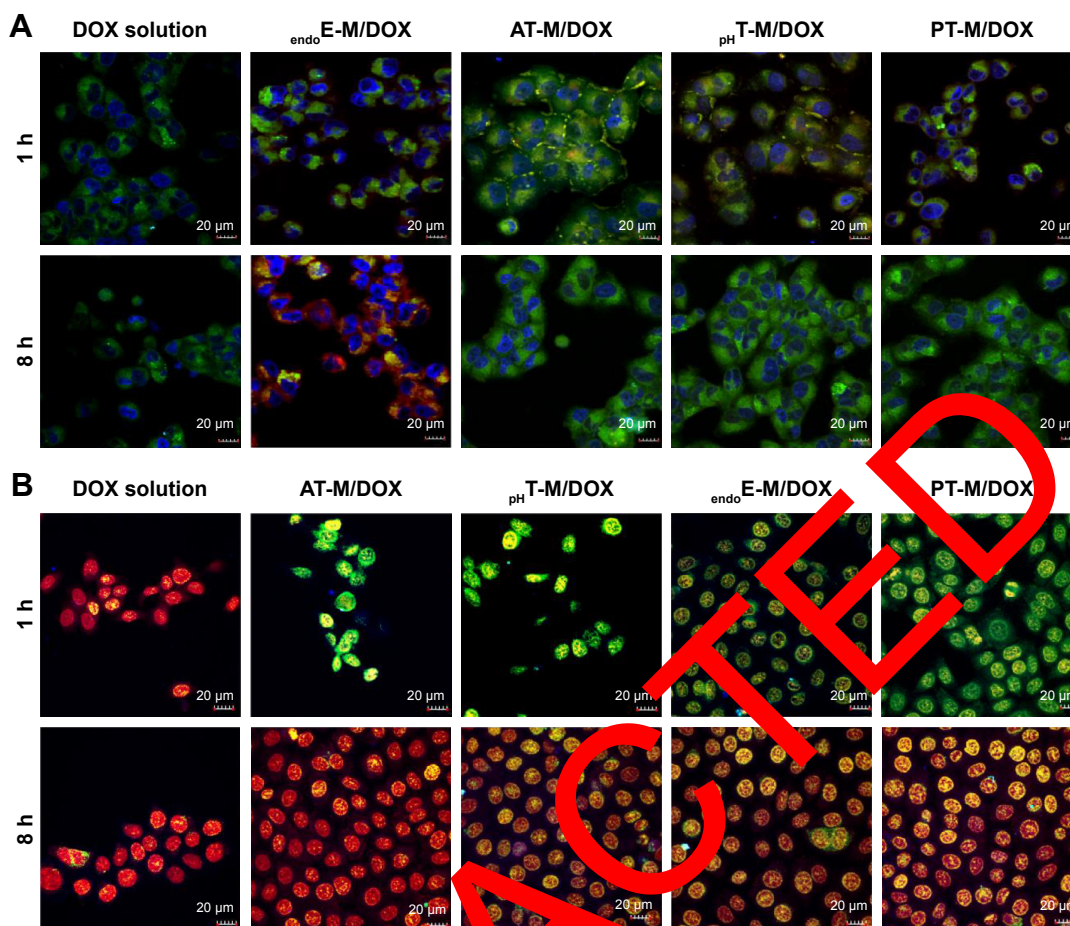
Figure 10 The confocal microscopic images of endosomal escape of AT-M/DOX, pHT-M/DOX, endoE-M/DOX and PT-M/DOX in MCF-7/ADR cells (**A**) and MCF-7 cells (**B**) at 37°C.
Notes: The cells were triple labeled with the nuclei selective dye (Hoechst 33258, blue), the dye selective for lysosomes (LysoTracker green) and anticancer drug (DOX, red). AT-M/DOX: DOX-incorporated micelles composed of FA-F127 (20% of Pluronic F127 conjugated with folate) and Pluronic P123 (w/w: 60/40) with active targeting. PT-M/DOX: DOX-incorporated micelles composed of Pluronic F127 and Pluronic P123 (w/w: 60/40) with passive targeting function. endoE-M/DOX: DOX-incorporated micelles composed of PHis-PLA-PEG-PLA-PHis and Pluronic F127 (w/w: 50/50) with endo-lysosomal escape. pHT-M/DOX: DOX-incorporated micelles composed of Pluronic P123 and Pluronic F127 (w/w: 90/10).
Abbreviation: DOX, doxorubicin.

cellular elimination after endocytosis, leading to enhanced DOX accumulation in DOX-resistant cancer cells and increased cytotoxicity. However, endosomal escape turned out to be an unnecessary function in treating DOX-sensitive cancer cells, suggesting a different intracellular pathway of NPs after endocytosis. 3) Active targeting and endosomal escape serve as a primary function to be integrated into delivery nanocarriers for treating drug-sensitive and drug-resistant cancer cells, respectively. 4) Triggered release can be served as an auxiliary function to further increase the payload concentration inside the cancer cells in a multiple functional delivery system.

Antitumor efficacy of different micelles

The in vivo antitumor efficacy of AT-M/DOX, endoE-M/DOX and PT-M/DOX was evaluated in the MCF-7 and MCF-7/ADR xenografted nude mice, respectively. The in vivo antitumor efficacy of pHT-M/DOX was not investigated due to

the low micellar stability upon dilution in the bloodstream.[46] The tumor volume change of MCF-7 xenografted nude mice and the final weight of tumors are shown in Figure 11A and B, respectively. All the DOX-incorporated micelles exhibited stronger TGI than DOX solution (Figure 11A). As shown in Table 2, among the tested micelles, AT-M/DOX demonstrated the strongest TGI, as characterized by a significantly higher TGI of 91.33%, compared to endoE-M/DOX (85.05%) and PT-M/DOX (81.27%; $P<0.05$, Table 4). The final tumor weight of AT-M/DOX-treated mice was 140.5±3.17 mg, which was approximately 1.2 and 1.3 times smaller than those treated with endoE-M/DOX and PT-M/DOX, respectively ($P<0.05$; Figure 11B). The antitumor results indicate the dominant role of active targeting in treating DOX-sensitive tumor, which was in accordance with the in vitro results. In addition, endoE-M/DOX and PT-M/DOX exhibited no significant difference in TGI due to similar passive targeting
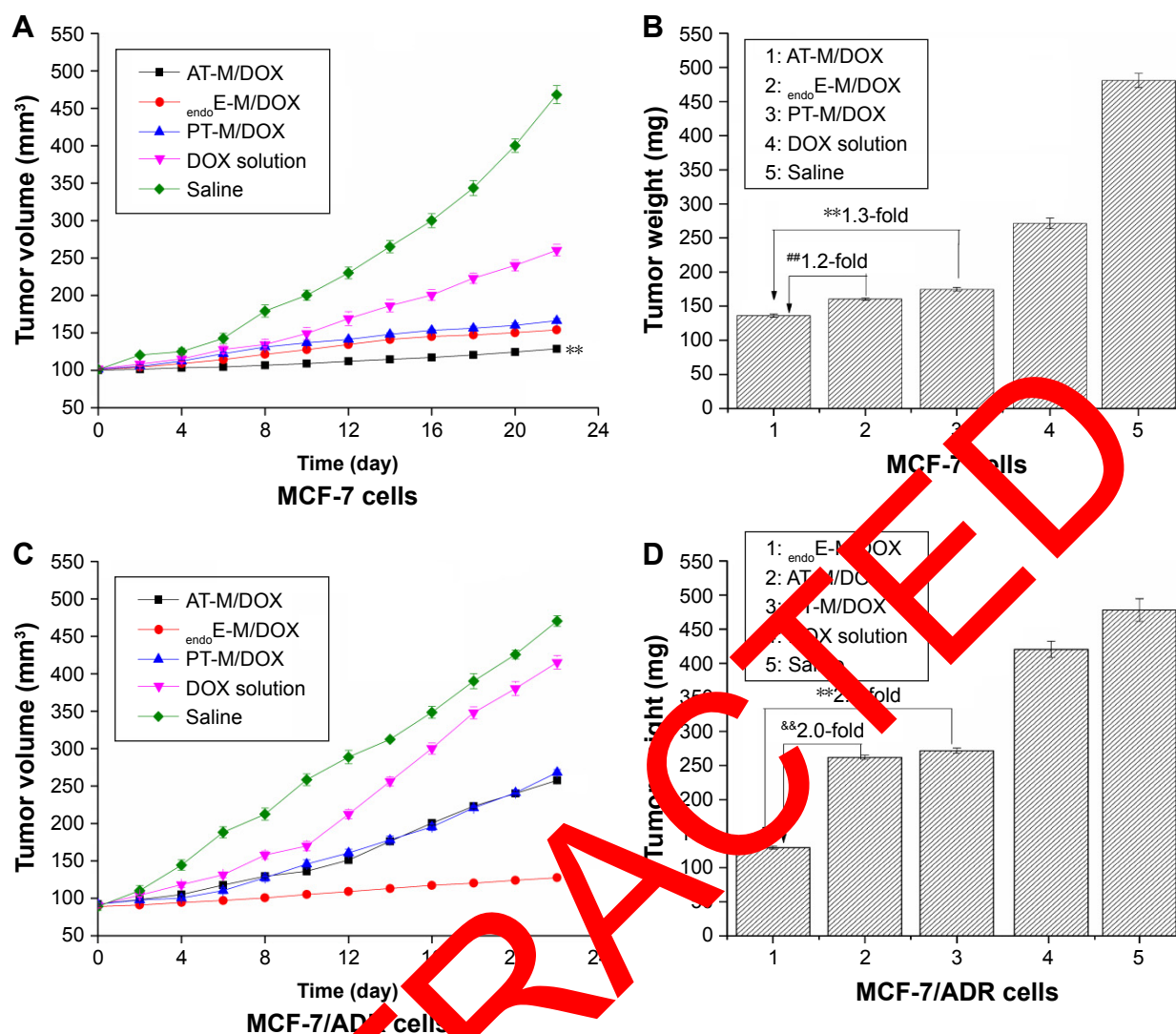
Figure 11 The tumor volume change of MCF-7 xenografted nude mice (**A**, n=7) and MCF-7/ADR xenografted nude mice (**C**, n=7) and the weights of excised tumors from MCF-7 xenografted nude mice (**B**, n=7) and MCF-7/ADR xenografted nude mice (**D**, n=7) post iv administration of saline, DOX solution, AT-M/DOX, endoE-M/DOX and PT-M/DOX.
Notes: **$P<0.05$: significantly different from PT-M/DOX. ##$P<0.05$: significantly different from endoE-M/DOX. &&$P<0.05$: significantly different from AT-M/DOX. AT-M/DOX: DOX-incorporated micelles composed of Pluronic F127 (20% of Pluronic F127 conjugated with folate) and Pluronic P123 (w/w: 60/40) with active targeting. PT-M/DOX: DOX-incorporated micelles composed of Pluronic F127 and Pluronic P123 (w/w: 60:40) with passive targeting function. endoE-M/DOX: DOX-incorporated micelles composed of PHis-PLA-PEG-PLA-PHis and Pluronic F127 (w/w: 50/50) with endo-lysosomal escape.
Abbreviations: DOX, doxorubicin; iv, intravenous.

property, indicating the unnecessary role of endo-lysosomal escape in treating DOX-sensitive tumor.

The tumor volume change of MCF-7/ADR xenografted nude mice and the final weight of tumors are shown in Figure 11C. DOX solution demonstrated a slightly lower TGI (15.35%) than saline, indicating failure of chemotherapy for the DOX-resistant tumor. All the DOX-incorporated micelles showed significantly higher TGI than DOX solution ($P<0.05$) because of the enhanced DOX accumulation in the tumor cells by different uptake pathways into DOX-resistant cells. Among the tested micelles, endoE-M/DOX

demonstrated the strongest TGI, as characterized by the significantly higher TGI of 90.33%, compared to AT-M/DOX (56.82%) and PT-M/DOX (54.22%; $P<0.05$, Table 4). The final average tumor weight of endoE-M/DOX-treated mice was 129.43±2.17 mg, which was 2.0 and 2.1 times smaller than those treated with AT-M/DOX and PT-M/DOX ($P<0.05$; Figure 11D). In addition, AT-M/DOX showed no significant difference in TGI with PT-M/DOX ($P>0.05$). The antitumor results indicate that: 1) active targeting resulted in comparable therapeutic efficacy with passive targeting due to the elimination of DOX from the resistant tumor and

Table 4 TGI of DOX-incorporated micelles against MCF-7 and MCF-7/ADR xenografted nude mice (n=7)

Formulations	MCF-7 tumor volume (cm³)			MCF-7/ADR tumor weight (cm³)		
	Day (0, cm³)	Day (22, cm³)	TGI (%)	Day (0, cm³)	Day (22, cm³)	TGI (%)
endoE-M/DOX	104.3±1.76	174.9±1.29	81.27±1.24	92.1±2.13	123.4±1.85	90.33±1.08
AT-M/DOX	103.5±1.81	128.1±1.08	91.33±0.91	95.2±1.98	261.8±2.21	56.82±1.61
pHT-M/DOX	104.2±1.32	160.5±2.11	85.05±1.10	95.1±2.34	271.8±1.77	54.21±1.29
DOX solution	105.1±2.01	271.4±1.98	55.86±0.84	93.7±2.45	420.4±5.23	15.35±2.17
Saline	104.2±1.54	480.9±2.11	–	92.1±1.69	478.1±6.19	–

Notes: AT-M/DOX: DOX-incorporated micelles composed of Pluronic F127 (20% of Pluronic F127 conjugated with folate) and Pluronic P123 (w/w: 60/40) with active targeting. PT-M/DOX: DOX-incorporated micelles composed of Pluronic F127 and Pluronic P123 (w/w: 60:40) with passive targeting function. endoE-M/DOX: DOX-incorporated micelles composed of PHis-PLA-PEG-PLA-PHis and Pluronic F127 (w/w: 50/50) with endo-lysosomal escape.
Abbreviations: DOX, doxorubicin; TGI, tumor growth inhibition.

2) endo-lysosome escape played a dominant role in sparing DOX elimination from the resistant tumor, leading to the strongest therapeutic efficacy.

The body weight change of the different mice groups is shown in Figure 12. Mice treated with DOX solution exhibited nearly 30% decrease in weight in both MCF-7 group and MCF-7/ADR group; with a bad physical condition, even death occurred, indicating the severe systemic toxicity of DOX solution. Compared to DOX solution, mice treated with all the micelles did not show obvious weight loss. In addition, mice treated with endoE-M/DOX showed no significant weight loss compared to those treated with AT-M/DOX (*P*>0.05), indicating the comparable safety shown by Pluronic micelles.

Conclusion

In this study, four kinds of micelles with active-targeting (AT-M), stimuli-triggered release (pHT-M) and endo-lysosomal escape (endoE-M) were constructed to elucidate the therapeutic efficacy of four individual functions (active targeting, passive targeting, stimuli-triggered release and endo-lysosomal escape) against DOX-sensitive MCF-7 cells and DOX-resistant MCF-7/ADR cells, respectively. Effectively enhanced drug accumulation in the cancer cells has been proven to be an ideal approach to design a multifunctional nanocarrier against MCF-7 sensitive cells. However, this approach failed to demonstrate significant therapeutic efficacy to the MCF-7/ADR cells due to the remarkable difference in cellular elimination of the two cell lines. Endo-lysosomal
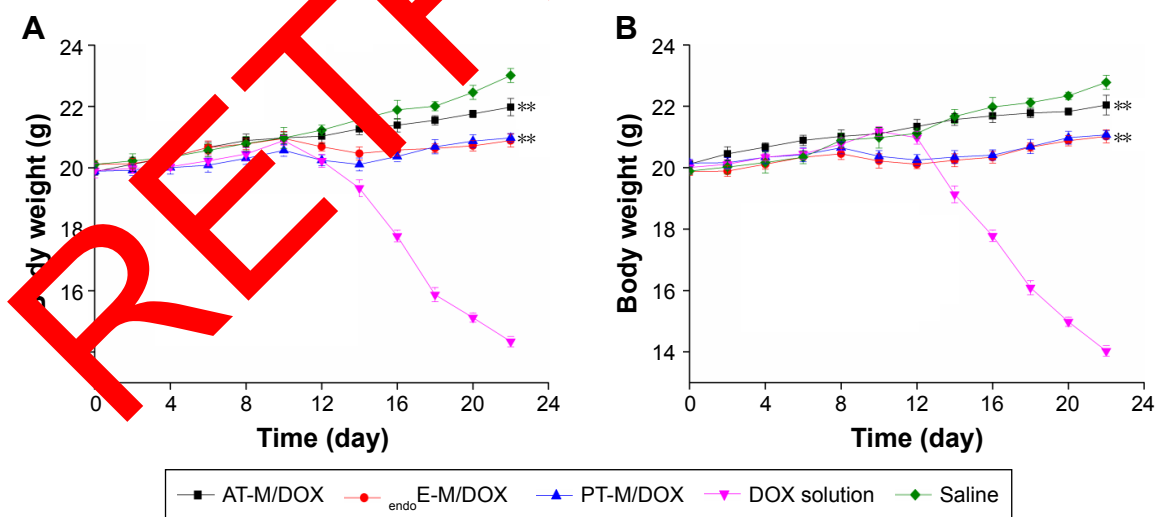

Figure 12 The variation of body weights of MCF-7/ADR xenografted nude mice post iv injection of saline, DOX solution, AT-M/DOX, endoE-M/DOX and PT-M/DOX (**A**, n=7). The variation of body weights of MCF-7 xenografted nude mice post iv injection of saline, DOX solution, AT-M/DOX, endoE-M/DOX and PT-M/DOX (**B**, n=7).
Notes: **P*<0.05: significantly different from DOX solution. AT-M/DOX: DOX-incorporated micelles composed of Pluronic F127 (20% of Pluronic F127 conjugated with folate) and Pluronic P123 (w/w: 60/40) with active targeting. PT-M/DOX: DOX-incorporated micelles composed of Pluronic F127 and Pluronic P123 (w/w: 60:40) with passive targeting function. endoE-M/DOX: DOX-incorporated micelles composed of PHis-PLA-PEG-PLA-PHis and Pluronic F127 (w/w: 50/50) with endo-lysosomal escape.
Abbreviations: DOX, doxorubicin; iv, intravenous.

escape has been proved to play a dominant role in sparing the payload elimination from MCF-7/ADR cells in order to achieve an effective delivery. This study has shed some light on what is a rational design for a multifunctional nanocarrier against MCF-7 and MCF-7/ADR cells. Of course, more studies are expected to testify these individual functions on other cancer cell lines in order to fully elucidate the rational design of multifunctional nanocarriers against drug-sensitive and drug-resistant cancer cells.

Acknowledgments

Disclosure

The authors report no conflicts of interest in this work.

References

1. Wang A, Chen L, Li C, Zhu Y. Heterogeneity in cancer stem cells. *Cancer Lett*. 2015;357(1):63–68.
2. Xiao Y, Hong H, Javadi A, et al. Multifunctional unimolecular micelles for cancer-targeted drug delivery and positron emission tomography imaging. *Biomaterials*. 2012;33(11):3071–3082.
3. Li X, Qian Y, Liu T, et al. Amphiphilic multiarm star block copolymer-based multifunctional unimolecular micelles for cancer targeted drug delivery and MR imaging. *Biomaterials*. 2011;32(27):6595–6605.
4. Li X, Yu Y, Ji Q, Qiu L. Targeted delivery of anticancer drugs by aptamer AS1411 mediated Pluronic F127/cyclodextrin-linked polymer composite micelles. *Nanomedicine*. 2015;11(1):175–184.
5. Qiu L, Qiao M, Chen Q, et al. Enhanced effect of pH-sensitive mixed copolymer micelles for overcoming multidrug resistance of doxorubicin. *Biomaterials*. 2014;35(37):9877–9887.
6. Milane L, Ganesh S, Shah S, Duan ZF, Amiji M. Multi-modal strategies for overcoming tumor drug resistance: hypoxia, the Warburg effect, stem cells, and multifunctional nanotechnology. *J Controlled Release*. 2011;155(2):237–247.
7. Zhang Y, Zhang H, Wang X, Wang J, Zhang X, Zhang Q. The eradication of breast cancer and cancer stem cells using octreotide modified paclitaxel active targeting micelles and salinomycin passive targeting micelles. *Biomaterials*. 2012;33(2):679–691.
8. Maeda H. The enhanced permeability and retention (EPR) effect in tumor vasculature: the key role of tumor-selective macromolecular drug targeting. *Adv Enzyme Regul*. 2001;41:189–207.
9. Fang J, Sawa T, Maeda H. Factors and mechanism of "EPR" effect and the enhanced antitumor effects of macromolecular drugs including SMANCS. *Adv Exp Med Biol*. 2003;519:29–49.
10. Tanaka T, Shiramoto S, Miyashita M, Fujishima Y, Kaneo Y. Tumor targeting based on the effect of enhanced permeability and retention (EPR) and the mechanism of receptor-mediated endocytosis (RME). *Int J Pharm*. 2004;277(1–2):39–61.
11. Fan L, Li F, Zhang H, et al. Co-delivery of PDTC and doxorubicin by multifunctional micellar nanoparticles to achieve active targeted drug delivery and overcome multidrug resistance. *Biomaterials*. 2010;31(21):5634–5642.

12. Zhao YZ, Dai DD, Lu CT, et al. Epirubicin loaded with propylene glycol liposomes significantly overcomes multidrug resistance in breast cancer. *Cancer Lett*. 2013;330(1):74–83.
13. Wang Y, Yu L, Han L, Sha X, Fang X. Difunctional Pluronic copolymer micelles for paclitaxel delivery: synergistic effect of folate-mediated targeting and Pluronic-mediated overcoming multidrug resistance in tumor cell lines. *Int J Pharm*. 2007;337(1–2):63–73.
14. Han M, Diao YY, Jiang HL, et al. Molecular mechanism study of chemosensitization of doxorubicin-resistant human myelogenous leukemia cells induced by a composite polymer micelle. *Int J Pharm*. 2011;420(2):404–411.
15. Kawaguchi T, Honda T, Nishihara M, Yamamoto T, Yokoyama M. Histological study on side effects and tumor targeting of a block copolymer micelle on rats. *J Control Release*. 2009;136(3):240–246.
16. Soga O, van Nostrum CF, Fens M, et al. Thermosensitive and biodegradable polymeric micelles for paclitaxel delivery. *J Control Release*. 2005;103(2):341–353.
17. Sawant RM, Hurley JP, Salmaso S, et al. "SMART" drug delivery systems: double-targeted pH-responsive pharmaceutical nanocarriers. *Bioconjug Chem*. 2006;17(4):943–949.
18. Rapoport N, Pitt WG, Sun H, Nelson JL. Drug delivery in polymeric micelles: from in vitro to in vivo. *J Control Release*. 2003;91(1–2):85–95.
19. Lee ES, Shin HJ, Na K, Bae YH. Poly(L-histidine)-PEG block copolymer micelles and pH-induced destabilization. *J Control Release*. 2003;90(3):363–374.
20. Lee ES, Na K, Bae YH. Polymeric micelle for tumor pH and folate-mediated targeting. *J Control Release*. 2003;91(1–2):103–113.
21. Lee ES, Oh KT, Kim D, Youn YS, Bae YH. Tumor pH-responsive flower-like micelles of poly(L-lactic acid)-b-poly(ethylene glycol)-b-poly(L-histidine). *J Controlled Release*. 2007;123(1):19–26.
22. Hong W, Chen D, Zhang X, et al. Reversing multidrug resistance by intracellular delivery of Pluronic(R) P85 unimers. *Biomaterials*. 2013;34(37):9602–9614.
23. Wang YY, Zhang DD, Kong YY, et al. CS/PAA@TPGS/PLGA nanoparticles with intracellular pH-sensitive sequential release for delivering drug to the nucleus of MDR cells. *Colloids Surf B Biointerfaces*. 2016;145:716–727.
24. Li J, Wang Y, Zhu Y, Oupicky D. Recent advances in delivery of drug-nucleic acid combinations for cancer treatment. *J Control Release*. 2013;172(2):589–600.
25. Xiong XB, Uludag H, Lavasanifar A. Biodegradable amphiphilic poly(ethylene oxide)-block-polyesters with grafted polyamines as supramolecular nanocarriers for efficient siRNA delivery. *Biomaterials*. 2009;30(2):242–253.
26. Torchilin VP. Targeted polymeric micelles for delivery of poorly soluble drugs. *Cell Mol Life Sci*. 2004;61(19–20):2549–2559.
27. Qu MH, Zeng RF, Fang S, Dai QS, Li HP, Long JT. Liposome-based co-delivery of siRNA and docetaxel for the synergistic treatment of lung cancer. *Int J Pharm*. 2014;474(1–2):112–122.
28. Shi C, Guo X, Qu Q, Tang Z, Wang Y, Zhou S. Actively targeted delivery of anticancer drug to tumor cells by redox-responsive star-shaped micelles. *Biomaterials*. 2014;35(30):8711–8722.
29. Dong D, Gao W, Liu Y, Qi XR. Therapeutic potential of targeted multifunctional nanocomplex co-delivery of siRNA and low-dose doxorubicin in breast cancer. *Cancer Lett*. 2015;359(2):178–186.
30. Zhang W, Shi Y, Chen Y, Ye J, Sha X, Fang X. Multifunctional Pluronic P123/F127 mixed polymeric micelles loaded with paclitaxel for the treatment of multidrug resistant tumors. *Biomaterials*. 2011;32(11):2894–2906.
31. Hong W, Chen D, Jia L, et al. Thermo- and pH-responsive copolymers based on PLGA-PEG-PLGA and poly(L-histidine): synthesis and in vitro characterization of copolymer micelles. *Acta Biomater*. 2014;10(3):1259–1271.

32. Netala VR, Bethu MS, Pushpalatha B, et al. Biogenesis of silver nanoparticles using endophytic fungus Pestalotiopsis microspora and evaluation of their antioxidant and anticancer activities. *Int J Nanomed*. 2016;11:5683–5696.

33. Mordant P, Loriot Y, Leteur C, et al. Dependence on phosphoinositide 3-kinase and RAS-RAF pathways drive the activity of RAF265, a novel RAF/VEGFR2 inhibitor, and RAD001 (Everolimus) in combination. *Mol Cancer Ther*. 2010;9(2):358–368.

34. Schmalenberg KE, Frauchiger L, Nikkhouy-Albers L, Uhrich KE. Cytotoxicity of a unimolecular polymeric micelle and its degradation products. *Biomacromolecules*. 2001;2(3):851–855.

35. Yin H, Lee ES, Kim D, Lee KH, Oh KT, Bae YH. Physicochemical characteristics of pH-sensitive poly(L-histidine)-b-poly(ethylene glycol)/poly(L-lactide)-b-poly(ethylene glycol) mixed micelles. *J Control Release*. 2008;126(2):130–138.

36. Zhang Y, Lam YM. Study of mixed micelles and interaction parameters for polymeric nonionic and normal surfactants. *J Nanosci Nanotechnol*. 2006;6(12):3877–3881.

37. Valiathan C, McFaline JL, Samson LD. A rapid survival assay to measure drug-induced cytotoxicity and cell cycle effects. *DNA Repair (Amst)*. 2012;11(1):92–98.

38. Kim JJ, Tannock IF. Repopulation of cancer cells during therapy: an important cause of treatment failure. *Nat Rev Cancer*. 2005;5(7): 516–525.

39. Oh N, Park JH. Endocytosis and exocytosis of nanoparticles in mammalian cells. *Int J Nanomedicine*. 2014;9(Suppl 1):51–63.

40. Shen Y, Tang H, Zhan Y, Van Kirk EA, Murdoch WJ. Degradable poly(beta-amino ester) nanoparticles for cancer cytoplasmic drug delivery. *Nanomedicine*. 2009;5(2):192–201.

41. Chen R, Khormaee S, Eccleston ME, Slater NK. The role of hydrophobic amino acid grafts in the enhancement of membrane-disruptive activity of pH-responsive pseudo-peptides. *Biomaterials*. 2009;30(10): 1954–1961.

42. Bae Y, Fukushima S, Harada A, Kataoka K. Design of environment-sensitive supramolecular assemblies for intracellular drug delivery: polymeric micelles that are responsive to intracellular pH change. *Angew Chem Int Ed Engl*. 2003;42(38):4640–4643.

43. Mohajer G, Lee ES, Bae YH. Enhanced intercellular retention activity of novel pH-sensitive polymeric micelles in wild and multidrug resistant MCF-7 cells. *Pharmaceutical Res*. 2007;24(9):1618–1627.

44. Lee ES, Gao Z, Kim D, Park K, Kwon IC, Bae YH. Super pH-sensitive multifunctional polymeric micelle for tumor pH(e) specific TAT exposure and multidrug resistance. *J Control Release*. 2008;129(3): 228–236.

45. Kim D, Lee ES, Park K, Kwon IC, Bae YH. Doxorubicin loaded pH-sensitive micelle: antitumoral efficacy against ovarian A2780/DOXR tumor. *Pharmaceutical Res*. 2008;25(9):2074–2082.

46. Wang Y, Hao J, Li Y, et al. Poly(caprolactone)-modified Pluronic P105 micelles for reversal of paclitaxel resistance in SKOV-3 tumors. *Biomaterials*. 2012;33(18):4741–4751.